Machine Vision and Applications
DOI 10.1007/s00138-009-0223-x

ORIGINAL PAPER

Decision tree-based contrast enhancement for various color images

Chun-Ming Tsai · Zong-Mu Yeh · Yuan-Fang Wang

Received: 15 March 2008 / Revised: 8 October 2008 / Accepted: 30 July 2009

Abstract Conventional contrast enhancement methods are application-oriented and they need transformation functions and parameters which are specified manually. Furthermore, most of them do not produce satisfactory enhancement results for certain types of color images: dark, low-contrast, bright, mostly dark, high-contrast, and mostly bright. Thus, this paper proposes a decision tree-based contrast enhancement algorithm to enhance the above described color images simultaneously. This method includes three steps: first, statistical image features are extracted from the luminance distribution. Second, a decision tree-based classification is proposed to divide the input images into dark, low-contrast, bright, mostly dark, high-contrast, and mostly bright categories. Finally, these image categories are handled by piecewise linear based enhancement method. This novel enhancement method is automatic and parameter-free. Our experiments included different color and gray images. Experimental results show that the performance of the proposed enhancement method is better than other available methods in skin detection, visual perception, and image subtraction measurements.

Keywords Contrast enhancement · Piecewise linear transformation · Decision tree-based classification · Parameter-free enhancement · Color images

C.-M. Tsai (✉)
Department of Computer Science, Taipei Municipal University of Education, No. 1, Ai-Kuo W. Road, Taipei 100, Taiwan, ROC
e-mail: cmtsai@tmue.edu.tw

Z.-M. Yeh
Department of Mechatronic Technology, National Taiwan Normal University, Taipei 106, Taiwan, ROC

Y.-F. Wang
Department of Computer Science, University of California, Santa Barbara, CA 93106, USA

1 Introduction

Contrast enhancement techniques are designed to adjust the quality of an image for better human visual perception [1–3]. It is a very important preprocessing step for tasks in the image processing, video processing, medical image processing, aerial image processing, and computer vision. The enhancement methods can be further classified into six groups [1–3]: (1) spatial domain techniques [1–3], (2) frequency domain techniques [1–3], (3) color image processing techniques [3–8], (4) physics-based techniques [9], (5) fuzzy set techniques [10], and (6) hybrid techniques. However, most of these techniques are application-oriented. Furthermore, the above described methods may have difficulty enhance multiple types of color images simultaneously. Thus, we extend point processing of the spatial domain techniques to color image processing, and propose a decision-based contrast enhancement algorithm to enhance various color images simultaneously.

Contrast enhancement algorithms based on the spatial domain techniques can be divided into three main types: global, local, and hybrid. Global enhancement methods enhanced the image from the information (luminance and saturation) of an entire image. Mlsna and Rodriguez [11] proposed a histogram explosion method to enhance geoscience and remote sensing color image. Duan and Qiu [12] divided the luminance range [0, 255] into 256 intervals using a hierarchical division procedure and used a control parameter to control the mapping. Sun et al. [13] proposed a dynamic specific histogram algorithm to perform contrast enhancement for a real-time system due to its simplicity. Local enhancement methods enhanced the image for each pixel according to the information (luminance, saturation, and Retinex) of its own and its neighbor. Chatterji and Murthy [14] proposed an adaptive contrast enhancement method for color images. However, in their method, two parameters (e.g., enhancement

Published online: 30 September 2009

function and region size) need to be determined. Meylan and Süsstrunk [15] used a Retinex-based adaptive filter to enhance natural color images, and their results showed that the color image with halo area could be enhanced. However, it needed to choose the appropriate filter size to reduce halos images and to introduce global tone mapping for extremely high dynamic range images. Munteanu and Rosa [16] used GA algorithm to search the parameters of the Multi-Scale Retinex model and 11 parameters (e.g., seven for Retinex, four for GA) are needed to be set. Hybrid enhancement methods combined both global and local approaches. In these methods, an image is divided into non-overlay or overly regions and each region is conquered by global methods. Pei et al. [8] used color contrast enhancement based on saturation and adaptive histogram equalization (HE) based on luminance for ancient Chinese paintings. However, their method needed to determine a positive factor for controlling the luminance level and the window size of the adaptive HE. It is worth noting that global methods are simple and fast, and can be applied by simple hardware and processed in a real time system. Local methods yield better experimental results, but are slower than global methods. Hybrid methods have better experimental results, but are slower than global methods. In this paper, our method is a global method which is based on image content analysis, and it can achieve to be simple and fast.

Furthermore, no single enhancement scheme gives satisfactory results on six kinds of images such as images with dark color (e.g., foreground and background are concentrated and both are located at dark illumination), images with bright color (e.g., foreground and background are concentrated and both are located at bright illumination), images with low-contrast (e.g., foreground and background are concentrated and both are located at middle illumination), images with major dark color and minor bright color, images with major bright color and minor dark color, and images with high-contrast (e.g., foreground and background color are spread from dark to bright illumination). Most current methods fail to provide good and efficient enhancement results. Moreover, the conventional enhancement methods require human assistance in determining the enhancement transformation function and parameters. Therefore, the objective of this paper is to propose a method that can process these six kinds of color images simultaneously. Moreover, the proposed method can automatically define the enhancement transformation function, and the parameters of the transformation function are chosen automatically. In other words, it is parameter-free, and it does not require the intervention by a human operator. This enhancement method, moreover, can be applicable to a variety of images, including face images, car images, bio images, medical images, aerial images and space images.

Figure 1 illustrates the proposed system flow diagram. A color image is initially transformed into the luminance spaces. Then, the luminance histogram is computed and a Gaussian smoothing filter is employed to remove unreliable peaks and valleys in the histogram. Next, the entire image distribution is analyzed to extract statistical features, they are used to classify input images as a tree structure, and the tree leaf nodes include the six kinds of images. Furthermore, the automatic and parameter-free piecewise linear enhancement method is used to enhance the images. Finally, the backward color transformation is applied to produce the enhancement result.

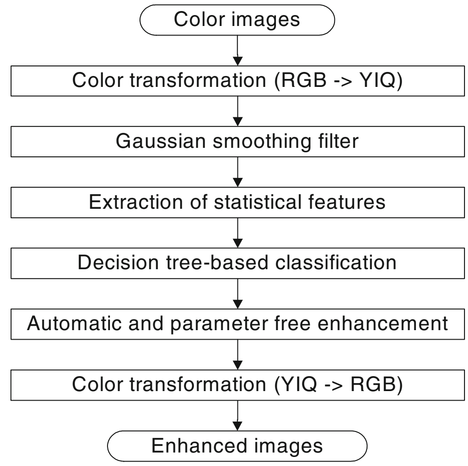

Fig. 1 Flow diagram of the proposed system

The remainder of this paper is organized as follows. Section 2 presents the preprocessing step. The decision tree-based classification algorithm will be described in Sect. 3. Section 4 explains the automatic and parameter free image enhancement algorithm. Section 5 discusses the experimental results. Finally, Sect. 6 contains concluding remarks and suggestions for future works.

2 Preprocessing

A robust image enhancement system must process both color and gray-level images. Hence, to enhance color images, transform to gray-level image is applied first. Then, an enhancement module is applied. Moreover, to apply the enhancement module to a wide range of applications, a classification module must be used to divide the color image into several subclasses. Finally, these subclasses are conquered by our proposal image enhancement algorithm. Herein, the preprocessing for the decision tree classifier and enhancement will be described first.

2.1 Color transformation

There are many color models [1,2,7,17]. In this paper, the input color image with *RGB* color model is adopted. Next, the

RGB color model is transformed to *YIQ* color model.To compute the luminance for an input color image, first, luminance Y (In the following, we use symbol L instead of symbol Y.) is used. Then, the luminance histogram $H_L(x)$ is computed, where the number of pixels with the various levels of brightness from black to white is shown. The histogram represents a probability distribution of the brightness levels. Finally, to obtain reliable peaks and valleys, a Gaussian smoothing filter is applied to smooth the original histogram, thus the unreliable peaks and valleys are removed.

2.2 Gaussian smoothing filter

The Gaussian convolution of a luminance histogram $H_L(x)$ depends upon both x and σ_g, namely, the Gaussian standard deviation. The convolution function $S_{HL}(x, \sigma_g)$ is provided by Eq. (1),

$$\begin{aligned} S_{HL}(x, \sigma_g) &= H_L(x) * g(x, \sigma_g) \\ &= \int_{-\infty}^{\infty} H_L(u) g(x-u, \sigma_g) \mathrm{d}u \\ &= \int_{-\infty}^{\infty} H_L(u) \frac{1}{\sqrt{2\pi}\sigma_g} \mathrm{e}^{-\frac{(x-u)^2}{2\sigma_g^2}} \mathrm{d}u, \end{aligned} \tag{1}$$

where "*" denotes the convolution operator and $g(x-u, \sigma_g)$ is the Gaussian function. The degree of smoothing is controlled by the standard deviation of the Gaussian function. The larger the standard deviation σ_g is, the smoother the function $S_{HL}(x, \sigma_g)$ is. Notably, in Tsai [18] the smoothing parameter is predetermined. In Tsai and Lee [17], they proposed the standard deviation which is decided automatically. This method is briefly as follows.

Standard deviation σ_g is based upon the majority of the widths within the luminance histogram. In a histogram $H_L(x)$, if $H_L(x) < H_L(x-1)$ and $H_L(x) < H_L(x+1)$, then luminance x is a valley. The highest point between two successive valleys is a peak, which identifies a distribution. Therefore, the widths between two successive valleys are computed and thus, the maximum width, $W_{\max}$, among the widths is determined. Next, the width histogram for all peaks from 0 to $W_{\max}$ is computed. After the highest point in the width histogram is located, which is regarded as the standard deviation σ_g of the widths, Eq. (1) is employed to convolute the histogram $H_L(x)$ that provides smoothing histogram.

2.3 Selection of image color distribution

Here one condition is assumed that color distributions in images are multi-Gaussian. Each color distribution can be represented by one peak and two valleys in luminance domain. Thus, the color distribution is selected by following algorithm. After the small peaks and valleys have been removed, the average differences are employed as the first derivation to determine the major peaks and valleys. The average difference in point x is defined by

$$S'_{HL}(x) = \frac{1}{\sigma_g - 1} \sum_{i=1}^{\sigma_g - 1} \frac{S_{HL}(x+i) - S_{HL}(x-i)}{2 \times i}. \tag{2}$$

A peak is defined as a positive to negative crossover in the first derivation of the smoothed histogram. Furthermore, a valley is defined as a negative to positive crossover. All peaks and valleys from the first derivation of the smoothed histogram are discovered. In cases where the peaks and valleys are too close, they will be removed if the distance between a valley and a peak is less than the standard deviation σ_g. The remaining peaks are the candidates of the luminance distribution in the image.

3 The decision tree-based classification

No single enhancement method can give satisfactory results on a variety type of images. For example, low-contrast image can be enhanced which produces pretty good result by contrast stretching (CS) method. But for the other type (dark, bright, mostly dark, high-contrast, and mostly bright) images, the CS method cannot produce satisfactory enhancement results. HE can enhance images with dark, low-contrast, bright, and high-contrast illumination [1]. But this method cannot enhance mostly dark and mostly bright images to obtain satisfactory results. Also, the result of HE produced annoying side effects [13]. Thus, a decision tree-based classification method is proposed to divide the input images into the six kinds of images and to enhance them, respectively.

3.1 Defining features

Based upon the luminance distribution, two statistical features are defined and used to classify the input images as one of the six kinds of images shown in Fig. 2. These two features are defined as follows.

1. The luminance variance, σ, of the entire image distribution: This feature describes whether the luminance distribution of the entire image is wide or narrow. Herein, the luminance variance, σ, represents the normalization variance which the range is from 0 to 255.
2. The luminance mean, μ, of the entire image distribution: This feature is used to locate the center-of-gravity position of the entire image distribution.

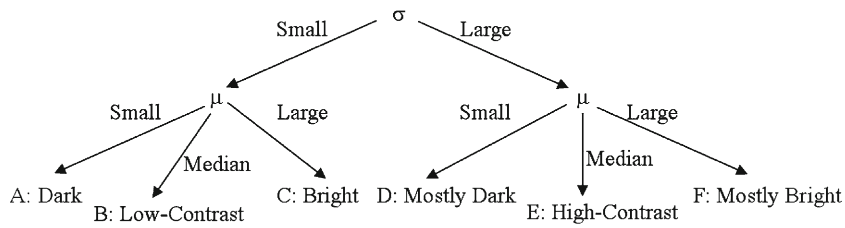

Fig. 2 Diagram of the decision tree-based classification to classify the input images into the six kinds of images

3.2 The decision tree

Figure 2 illustrates the diagram of the decision tree-based classification, which displays six image cases. The decision tree-based classification for the six kinds of images is shown in Table 1. For example, Case A is the dark image, if the luminance variance, σ, of the entire image is small and the luminance mean, μ, of the entire image is located at dark (small) illumination. Low-contrast image belongs to Case B if the luminance variance, σ, of the entire image is small and the luminance mean, μ, of the entire image is located at median illumination. Finally, Case F is part of minor dark and major bright image, if the luminance variance, σ, of the entire image is large and the luminance mean, μ, of the entire image is located at bright (large) illumination. The values of the small and large for the luminance variance, and the small, median, and large illuminations of the luminance mean will be described as follows.

3.3 Training the measure for the decision tree

Herein, 1,640, 300, 80, 3,021, 34,903, and 349 images which belong to case A, B, C, D, E, and F in the training set were employed, respectively. The training procedures applied to compute the ranges of the luminance variance, σ, are described as follows. (1) Compute the luminance variance, σ, for all training images. (2) Obtain the variance histogram from all training images. (3) Employ the Gaussian smoothing filter (Eq. 1) to smooth the variance histogram. (4) Achieve the peaks by using Eq. (2). (5) Select the middle between the first peak and second peak as the threshold value. Figure 3 illustrates the variance measure of the training procedure for the first level of the decision tree. Herein, the small ranges of the luminance variance were between 0 and 89. The large ranges of the luminance variance were between 89 and 255.

The decision tree first divided the input images into two image classes: small and large by the variance feature. To decide which image belonged to dark, median, or bright illumination, we divided the illumination into three parts such as dark, median, and bright. The illumination range of the dark part is from 0 to 85. The illumination between 86 and 175 belongs to the median part. The other belongs to the bright part. If the luminance mean of the input is belonged to dark, median, or bright parts, the input image will be set as the dark, median, or bright image, respectively.

4 Automatic and parameter free enhancement

The proposed enhancement algorithm is based on piece-wise linear transformation (PLT) [1,2,19]. The axiom of piece-wise linear transformation and how to build transformation function and parameters automatically are described as follows.

4.1 Piecewise linear transformation function

The PLT is characterized by $2k$ parameters for $k-1$ line segments. When the parameters are given, the transformation line segments will be determined. That is, if given the starting position of input luminance $\{x_k, k = 0, 1, \ldots, k\}$ and the starting position of output luminance $\{y_k, k = 0, 1, \ldots, k\}$, the $k-1$ transform functions $T_{k-1}(x)$ will be:

$$T_{k-1}(x) = \frac{(y_k - y_{k-1})}{(x_k - x_{k-1})} \cdot (x - x_{k-1}) + y_{k-1}. \tag{3}$$

Table 1 The decision tree-based classification for the six kinds of images

Case	σ	μ	Image classes	Samples
A	Small	Small	Dark	1,640
B	Small	Median	Low-contrast	300
C	Small	Large	Bright	80
D	Large	Small	Mostly dark	3,021
E	Large	Median	High-contrast	34,903
F	Large	Large	Mostly bright	349

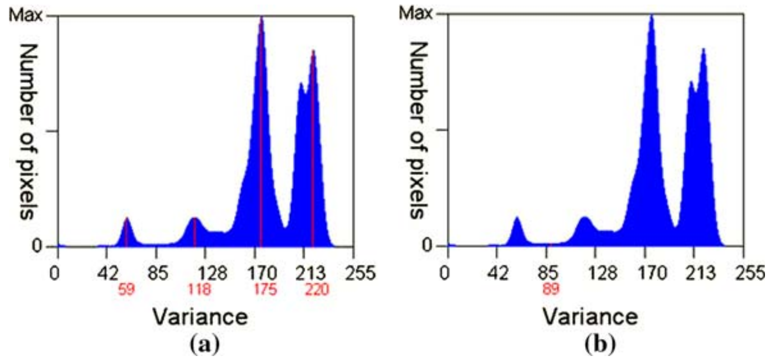

Fig. 3 Variance measure for the decision tree. **a** Four peaks are obtained from the luminance variance histogram. **b** Selecting the middle (89) between the first peak and the second peak as the threshold value

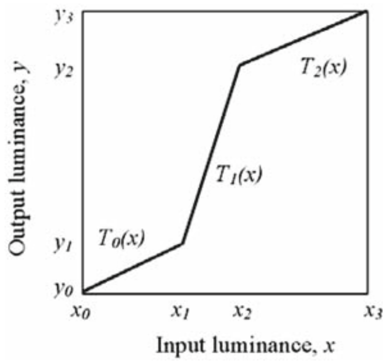

Fig. 4 Piecewise linear transformation function ($k = 3$, k is the number of the input parameters)

For example, if $k = 3$, form the $T_0(x)$, $T_1(x)$, and $T_2(x)$ transformation functions are shown in Fig. 4. Four input parameters and four output parameters will be specified first manually. To determine these parameters and line segments are critical for the satisfactory result of the contrast enhancement. In conventional applications, parameters and line segments are manually chosen case by case. To solve this problem, an automatic and parameter-free based contrast enhancement algorithm (APFCE) is proposed in the following.

4.2 Automatic and parameter-free based contrast enhancement

The proposed APFCE used the image content to determine the input and the output parameters. In Sect. 2, we have described that the input image is processed by transforming *RGB* into *YIQ*, getting the luminance histogram, smoothing the histogram, and selecting the color distributions. Each color distribution is selected by one peak and two valleys. Figure 5 shows an example for these processes. The original histogram is shown in Fig. 5a. Figure 5b is the smoothed histogram, which uses the Gaussian smoothing filter to smoothen Fig. 5a. The selection of the luminance distribution is depicted in Fig. 5c. There are five luminance distributions. The range of each luminance distribution is represented by one peak and its two valleys.

How is the number of line segments selected? The number of the image luminance distribution is used to represent the number of the line segments. If the number of the image luminance distribution is k, then the number of the line segment is $k+1$. How is the input luminance parameter decided? The location of the valley is used to represent the input luminance parameter, and different images may have different distribution of valleys. For example, there are five line segments in Fig. 5c. The input luminance parameters are 0, 56, 110, 151, 186, and 255. The location of these valleys and the parameters depend on what kind of image. How are the output luminance parameters determined? These parameters depend on what kind of the image, too. The determining method of input and output parameters are described in the following.

4.3 Decision tree-based image enhancement

From Table 1, images of Case A have two properties: (1) the center of gravity is located at dark illumination. (2) The luminance variance, σ, of the entire image is small, and it implies that the background and the foreground of the distribution is concentrated or narrow. These kind images were belonged to dark image. A transformation function is needed to transfer the dark and concentrated luminance distribution from dark spread to bright. The transformation function for Case A is designed as follows: If this kind of image has i luminance distributions $\{p_1, p_2, \ldots, p_i\}$ (peak is represented by p,) then the number of the line segment is $i+1$. Each distribution is bounded by two valleys indicated as v. That is, the i luminance distributions have $\{v_0, v_1, \ldots, v_i\}$ valleys. These valleys are used to be the input parameters $\{x_0, x_1, \ldots, x_i\}$ of the PLT function. The output parameters $\{y_0, y_1, \ldots, y_i\}$ of the PLT function is defined as follows:

$$y_0 = \sum_{x=s}^{p_1} \Pr(x) \cdot 255, \tag{4}$$

$$y_i = y_{i-1} + \sum_{x=v_{i-1}}^{v_i} \Pr(x) \cdot 255, \tag{5}$$

$$y_i = 255. \tag{6}$$

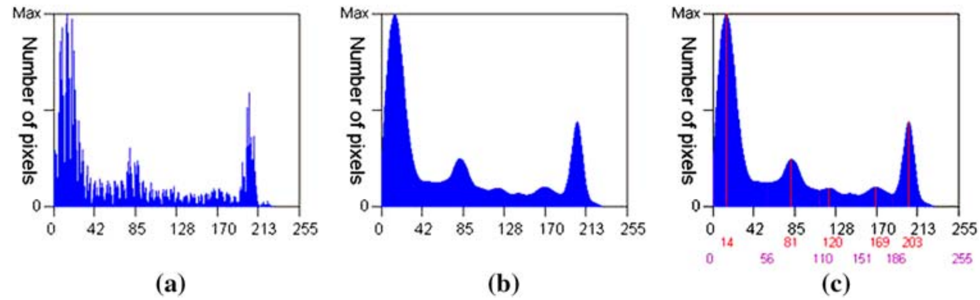

Fig. 5 An example for the preprocessing. **a** Original histogram. **b** Smoothed histogram. **c** Selection of image luminance distribution

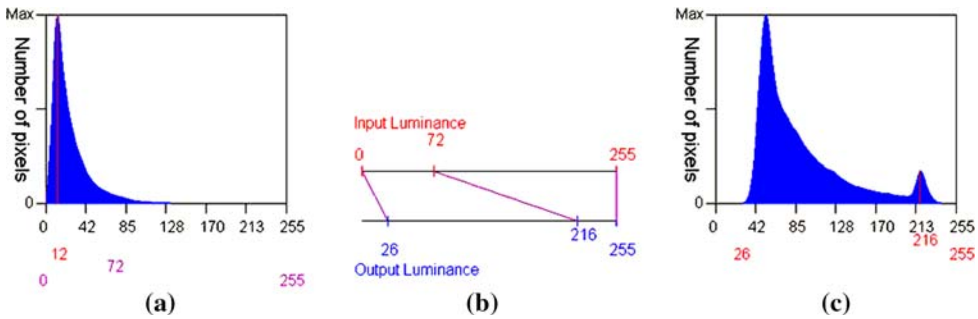

Fig. 6 An example for Case A (dark image). **a** Original smoothed histogram. **b** The input and output transformation. **c** The enhanced histogram

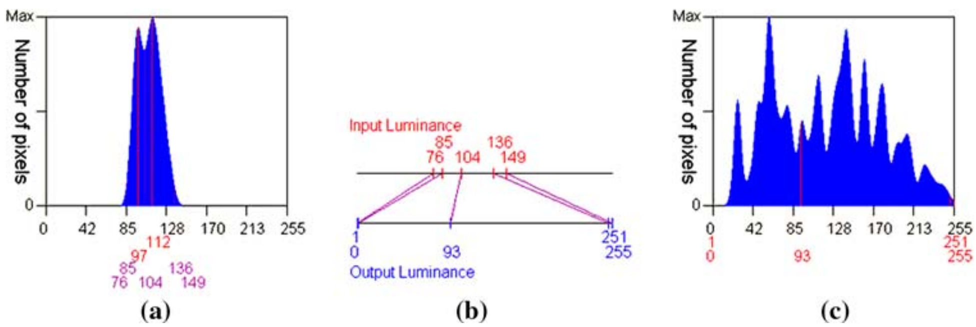

Fig. 7 An example for Case B (low-contrast image). **a** Original smoothed histogram. **b** The input and output transformation. **c** The enhanced histogram

where $Pr(x)$ is the probability of the luminance x. The parameter s is the start luminance of the input image. For human visual perception, the illumination value of black is smaller than 64 [17]. We adopt Eq. (4) to shift the darkest illumination to bright illumination. That is, the dark illumination can see more clearly. For example, if this kind of image has *one* luminance distribution $\{p_1\}$ which is represented by the foreground and background is concentrated or narrow. The valley is not easy to obtain. We adopt the Modified Triangle threshold method [17] to obtain a valley, and it is set as the threshold value T. That is, this kind of image has *two* line segments. The *one* luminance distribution has three valleys (e.g., $v_0 = s$, $v_1 = T$, $v_2 = e$), where s and e are indicated as the *start* and *end* luminance of the histogram, respectively. These valleys are used to be the input parameters $\{x_0, x_1, x_2\}$ of the PLT function.

Figure 6 gives an example for Case A with *one* concentrated foreground and background luminance distribution is located at dark illumination. Three input parameters (e.g., luminance values: 0, 72, 255) are shown in Fig. 6a. The luminance value 72 is obtained from Modified Triangle threshold method [17]. Figure 6b depicted the transformation in one-dimension, and the luminance values of output parameters are 26, 216, and 255. After enhancement, the image histogram is depicted in Fig. 6c. This figure also includes three output parameters (26, 216, and 255.)

Images of Case B have two properties. There are (1) the center of gravity is located at middle illumination. (2) The luminance variance, σ, of the entire image is small, which implies that the background and the foreground of the distribution is concentrated or narrow. These kind images were belonged to low-contrast image. The transformation function can transfer the low-contrast luminance distribution from median illumination to spread to dark luminance and bright luminance. Case B transformation function is designed as similar to Case A (by using Eqs. 4–6) except the output parameter $y_0 = 0$.

Figure 7 gives an example for Case B. This case has low-contrast luminance distribution. Five input parameters (luminance 76, 85, 104, 136, 149) are shown in Fig. 7a. The luminance 76 and 136 are obtained by the Modified Triangle threshold method [17]. The luminance 104 is obtained by

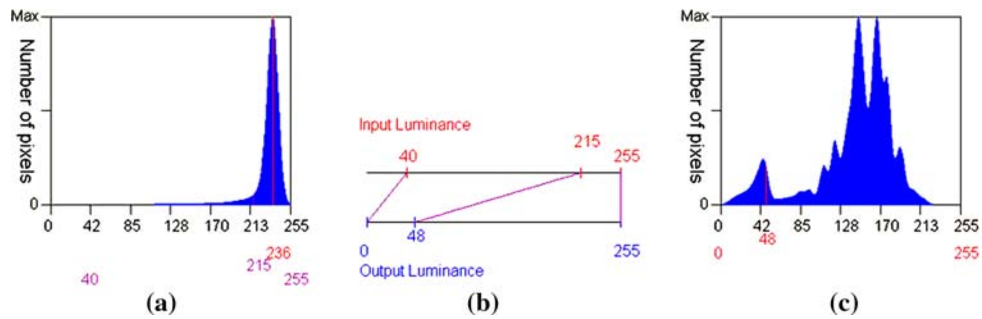

Fig. 8 An example for Case C (bright image). **a** Original smoothed histogram. **b** The input and output transformation. **c** The enhanced histogram

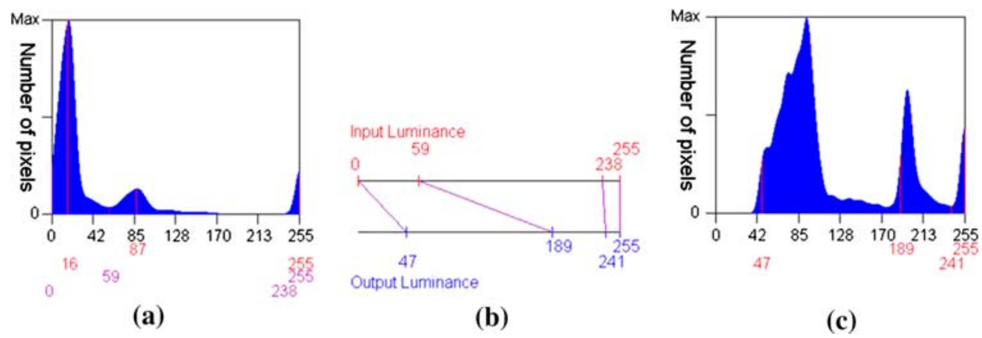

Fig. 9 An example for Case D (mostly dark image). **a** Original smoothed histogram. **b** The input and output transformation. **c** The enhanced histogram

the minimum luminance value between the two peaks (luminance 97 and 112). Figure 7b depicted the input and output transformation by one-dimension. After enhancement, the image histogram is depicted in Fig. 7c. This figure also includes five output parameters (luminance 0, 1, 93, 251, and 255).

There are two properties for images of Case C : such as the large mean, μ and the small luminance variance, σ, and it implies that the background and the foreground of the distribution is concentrated or narrow. These kind images were belonged to bright luminance distribution. To transfer the bright and concentrated luminance distribution from bright illumination spread to dark illumination. In this case, if we use the former formula to transform it, its results are too dark. This condition is owing to human visual perception. The different between bright luminance to dark luminance is too larger. That is, we introduce an *offset* parameter to resolve this problem. The *offset* parameter sets as maximum luminance minus mean luminance ($offset = 255 - ut$). Case C transformation function is designed as similar to Case A except the output parameters.

Figure 8 gives an example for Case C. Three input parameters (luminance 40, 215, and 255) are shown in Fig. 8a. The luminance value 215 is the threshold value which is obtained from Modified Triangle threshold method [17]. Figure 8b depicted the input and output transformation in one-dimension. After enhancement, the image histogram is depicted in Fig. 8c. This figure also includes three output parameters (luminance 0, 48, and 255).

Images of Case D have two properties such as the small mean, μ and the large luminance variance, σ, and it implies that the background and the foreground of the distribution is spread or wide. These properties imply that most of the luminance is located at dark illumination. The bright illuminations are minor. To spread the major dark illumination to bright illumination, a transformation function for Case D is defined as similar to Case A (by using Eqs. 4–6), but the preceding $k - 1$ valleys are obtained from the minimum luminance value between two neighbor peaks. For the kth valley, if the last peak is closed to luminance 255, it will set as 255; otherwise, it will set as a threshold value, which obtained from Modifies Triangle threshold method [17].

Figure 9 gives an example for Case D. Four input parameters (luminance 0, 59, 238, 255) are shown in Fig. 9a. The luminance values 59 and 238 are obtained from the minimum luminance value between two neighbor peaks. Figure 9b depicted the input and output transformation in one-dimension. After enhancement, the image histogram is depicted in Fig. 9c. This figure also has four output parameters (luminance 47, 189, 241, and 255.)

Images of Case E have two properties such as the median mean, σ and the large luminance variance, σ, and it implies that the background and the foreground of the distribution is spread or wide. These properties imply these kind images have high-contrast luminance distribution. In this case, the enhancement will be triggered by using Eqs. (4)–(6).

Figure 10 gives an example for Case E. Eight input parameters (luminance 1, 54, 99, 116, 145, 175, 240, 254) are shown in Fig. 10a. Figure 10b depicted the input and output transformation in one-dimension. After enhancement, the image histogram is depicted in Fig. 10c. This figure also includes

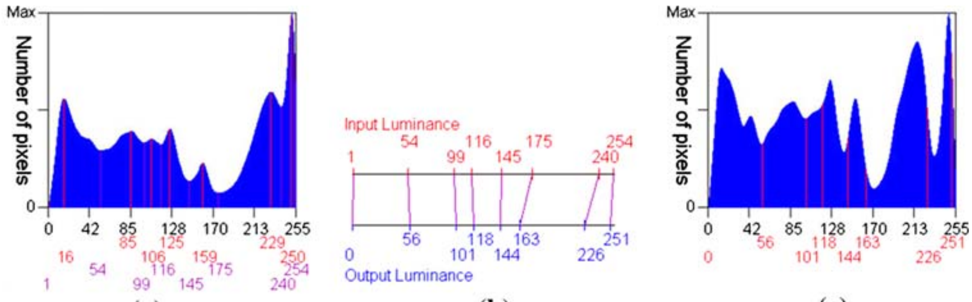

Fig. 10 An example for Case *E* (high-contrast image). **a** Original smoothed histogram. **b** The input and output transformation. **c** The enhanced histogram

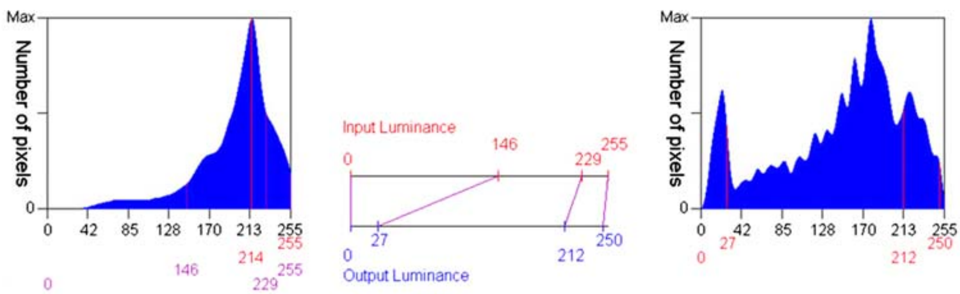

Fig. 11 An example for Case F (mostly bright image). **a** Original smoothed histogram. **b** The input and output transformation. **c** The enhanced histogram

Table 2 Summarize the examples for the decision tree-based image enhancement method

Case	σ	μ	Input parameters	Output parameters	Results
A	56.49	26.23	0, 72, 255	26, 216, 255	Fig. 12
B	28.90	108.76	76, 85, 104, 136, 149	0, 1, 93, 251, 255	Fig. 13
C	55.27	229.38	40, 215, 255	0, 48, 255	Fig. 14
D	177.24	52.56	0, 59, 238, 255	47, 189, 241, 255	Fig. 15
E	203.24	133.76	1, 54, 99, 116, 145, 175, 240, 254	0, 56, 101, 118, 144, 163, 226, 251	Fig. 16
F	101.43	196.29	0, 146, 229, 255	0, 27, 212, 250	Fig. 17

eight output parameters (luminance 0, 56, 101, 118, 144, 163, 226, 251).

Images of Case *F* have two properties: (1) the center of gravity is located at bright illumination. (2) The luminance variance, σ, of the entire image is large, this implies that the background and the foreground of the distribution is spread or wide. These properties imply that most of the luminance is located at bright illumination. The dark illuminations are minor. The transformation function must transfer the major bright illumination spread to dark illumination, a transformation function for Case *F* is defined as similar to Case *C* except that the *offset* parameter is cancel.

Figure 11 gives an example for Case *F*. Four input parameters (luminance 0, 146, 229, 255) are shown in Fig. 11a. Figure 11b depicted the input and output transformation in one-dimension. After enhancement, the image histogram is depicted in Fig. 11c. This figure also includes four output parameters (luminance 0, 27, 212, 250). The brightest illumination has been reduced, and the drawback of the HE enhancement method has been solved by this function.

Table 2 summarizes the examples for the decision tree-based image enhancement method. From this table, the output parameters are similar to the input parameters in Case *E* (high-contrast images). These images do not need to be enhanced in real applications.

5 Experimental results and discussion

The enhancement algorithm proposed for color images was implemented as a Windows-based application on a Pentium IV-1.7GHZ PC. Our experiments use various color and gray images. Most of the images are obtained from the book Digital Image Processing [1,2], Yale Face Database B [20], internet, and captured by ourselves. The images from the website of the "Digital Image Processing" have various kinds of images. These images include magnetic resonance images, aerial images, medical images, biomedical, and optical images, etc. The Yale Face Database B contains 5,760 single light source images of 10 subjects each seen under 576

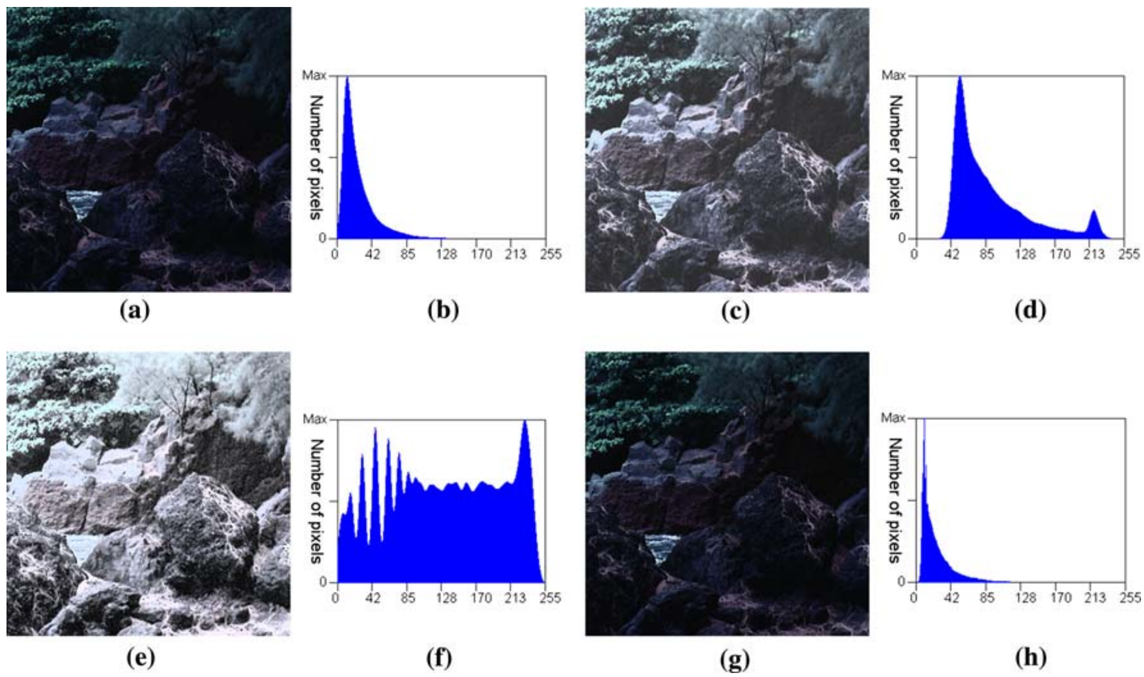

Fig. 12 Enhancement results for Case *A* (dark image). **a** Original color image. **b** The histogram of **a**. **c** Enhancement result by our proposal method. **d** The enhancement histogram of **c**. **e** Enhancement result by histogram equalization. **f** The enhancement histogram of **e**. **g** Enhancement result by contrast stretching. **h** The enhancement histogram of **g**

viewing conditions (9 poses $\times$ 64 illumination conditions). For every subject in a particular pose, an image with ambient (background) illumination was also captured. Hence, the total number images of Yale Face Database B are in fact 5,850. Some examples are presented as follows.

Figure 12 shows the enhancement results for Case *A*. From Fig. 12a, b, it is obvious that this color image with concentrated foreground and background distribution. This color image belongs to dark illumination. The result by the HE is improper. From Fig. 12e, the tree's and rock's color are distorted. Our result is less distortion (Fig. 12c). Notably, the HE result is brighter than ours by the comparison between Fig. 12d and f. The brighter effect makes the distortion. Our proposal enhancement can reduce the effect. Moreover, the HE enhances the color image from darkest illumination (0) to brightest illumination (255). This will produce the effect of intermittent illumination. That is, our result is better than that of HE. The result of the CS is shown in Fig. 12g. This result is similar to original image (Fig. 12a). The input parameters for CS are gray level 0 and 254. So, the enhanced result is not good. The CS cannot enhance the image with dark illumination.

The enhancement results for Case *B* are shown in Fig. 13. From Fig. 13a, b, it is obvious that the foreground and background of this image is concentrated. This image belongs to median illumination (low-contrast). The result by the HE is too brighter, and it has some foregrounds missed. These foregrounds are marked in Fig. 13c, e. The result (Fig. 13g) of the CS is similar to our result. Thus, the CS can enhance the image with low-contrast illumination. From these figures, our proposal image enhancement is better then HE does.

Figure 14 shows the enhancement results for Case *C*. From Fig. 14a, b, we know that the foreground and background of this image is concentrated. This image belongs to bright illumination. The result by the HE is brighter than our result. The result of the CS is shown in Fig. 14g. This result is similar to original image (Fig. 14a) and the enhancement result is failed. From the visual perception of these figures, our proposal image enhancement is better than HE and CS do. The CS cannot enhance the image with bright illumination.

The enhancement results for Case *D* are shown in Fig. 15. Figure 15a is obtained from the Yale Face Database B. This image belongs to subject #10 seen in pose #0, and the light source direction with respect to the camera axis is at 0° azimuth ("A+000") and 90° elevation ("E+90"). The most distribution of this image is dark illumination, and its bright illumination is minor. That is, the luminance variance is large, and the luminance mean is located at the dark illumination part. The eyes in Fig. 15e are not clear, and the hair and face are too bright. Our results of the eyes, hair, and face are better than those of HE. Although HE has a better result than ours regarding the wall, our proposed method is still better than HE. The result of the CS is shown in Fig. 15g,

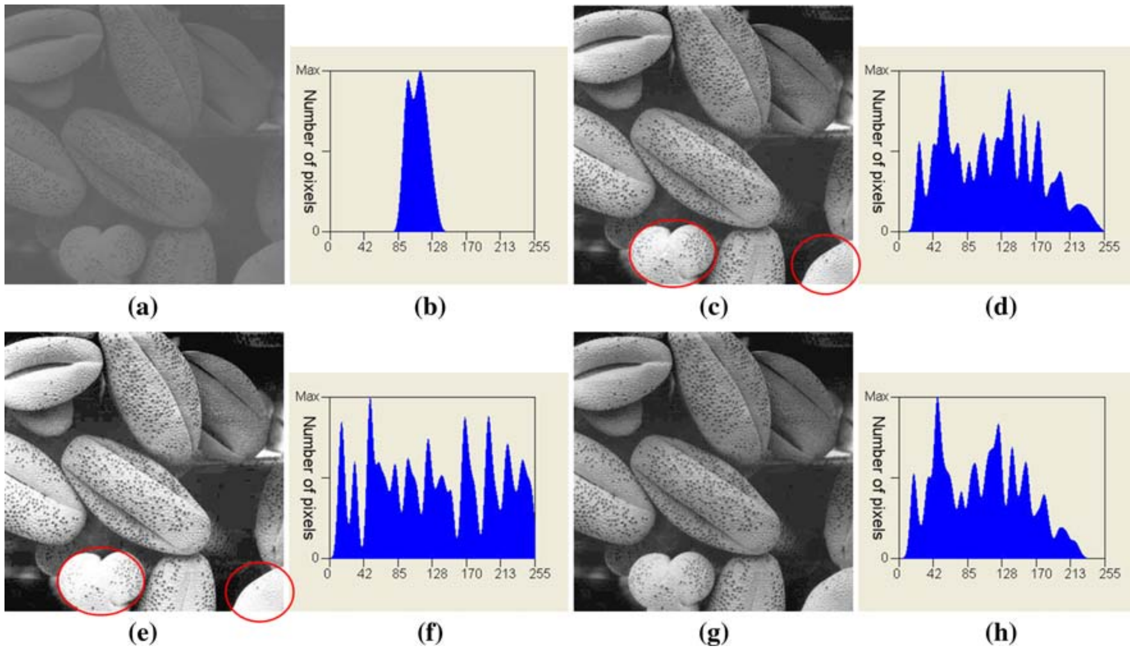

Fig. 13 Enhancement results for Case *B* (low-contrast image). **a** Original image. **b** The histogram of **a**. **c** Enhancement result by our proposal method. **d** The enhancement histogram of **c**. **e** Enhancement result by histogram equalization. **f** The enhancement histogram of **e**. **g** Enhancement result by contrast stretching. **h** The enhancement histogram of **g**

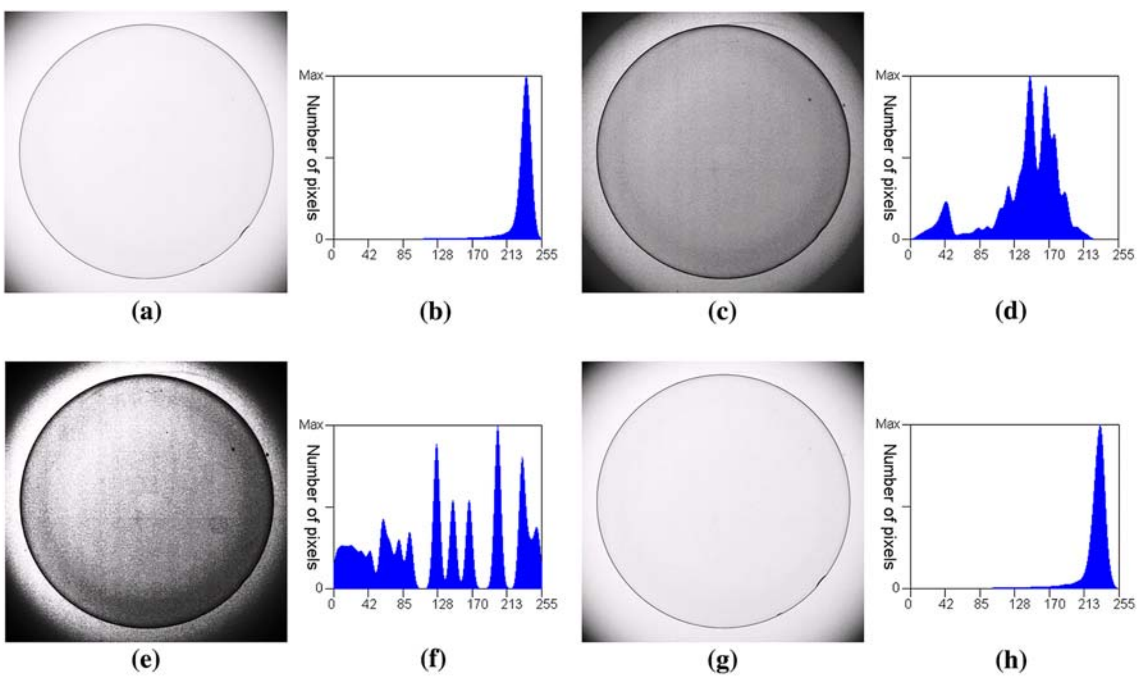

Fig. 14 Enhancement results for Case *C* (bright image). **a** Original image. **b** The histogram of **a**. **c** Enhancement result by our proposal method. **d** The enhancement histogram of **c**. **e** Enhancement result by histogram equalization. **f** The enhancement histogram of **e**. **g** Enhancement result by contrast stretching. **h** The enhancement histogram of **g**

and its result is similar to original image (Fig. 15a). Thus, the CS cannot enhance the image with mostly dark illumination.

Figure 16 shows the enhancement results for Case *E*. From Fig. 16a, b, the foreground and background of this image are scattered from dark to bright. The center-of-gravity position

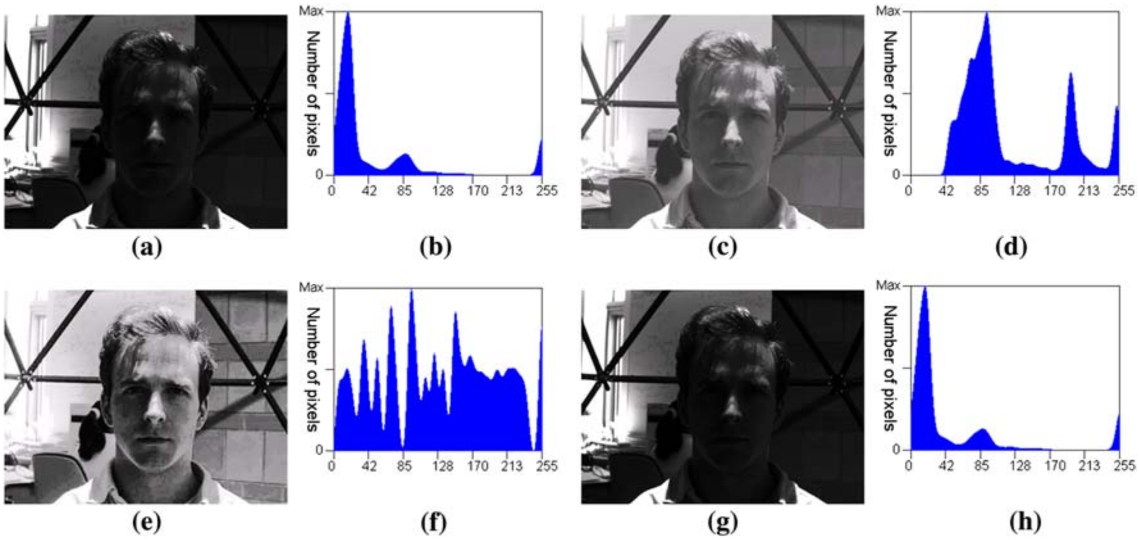

Fig. 15 Enhancement results for Case D (mostly dark image). **a** Original image. **b** The histogram of **a**. **c** Enhancement result by our proposal method. **d** The enhancement histogram of **c**. **e** Enhancement result by histogram equalization. **f** The enhancement histogram of **e**. **g** Enhancement result by contrast stretching. **h** The enhancement histogram of **g**

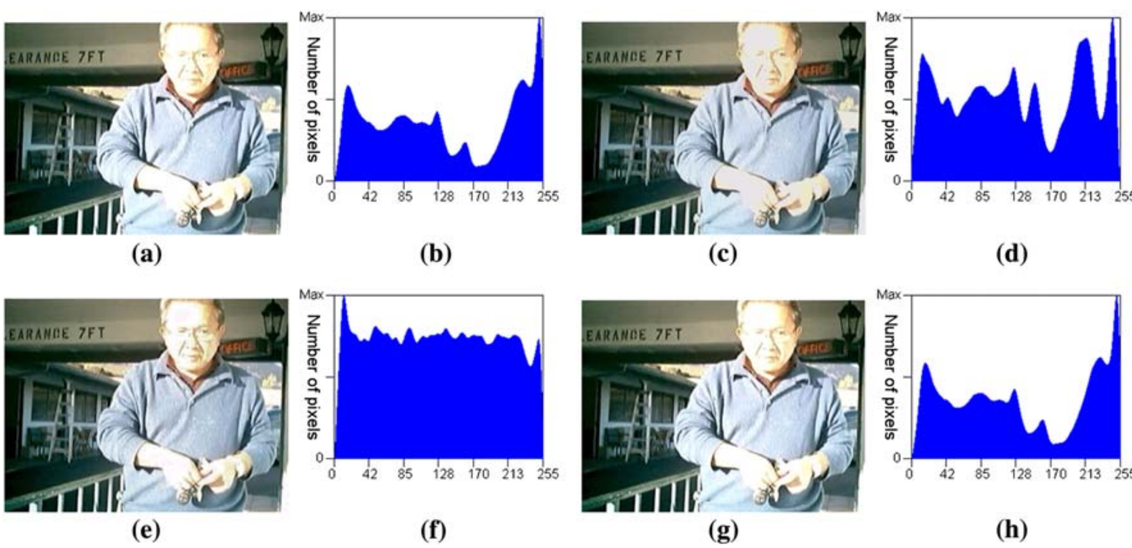

Fig. 16 Enhancement results for Case E (high-contrast image). **a** Original image. **b** The histogram of **a**. **c** Enhancement result by our proposal method. **d** The enhancement histogram of **c**. **e** Enhancement result by histogram equalization. **f** The enhancement histogram of **e**. The enhancement result by contrast stretching. **h** The enhancement histogram of **g**

is located at the median luminance. This kind of images belongs to high-contrast image. From Fig. 16e, f, the HE reduced the bright luminance part and enhanced the other part. Our proposed method reduced the brighter luminance part and enhanced the lower bright luminance part. From visual perception, both the proposal method and HE have similar performance. The result of the CS is shown in Fig. 16g. This result is similar to original image (Fig. 16a) and the enhancement result is failed. Thus, the CS cannot enhance the image with high-contrast illumination.

Figure 17 shows the enhancement results for Case F. From Fig. 17a, b, the foreground and background of this image dispersed from low to high luminance. The most distribution of this image is bright illumination, and its dark illumination is minor. That is, the luminance variance is large, and the luminance mean is located at the bright illumination part. This kind of image is belonged to minor dark and major bright illumination. From visual perception, both the proposal method and HE have similar performance. For CS, the result is shown in Fig. 17g which is similar to original image (Fig. 17a). From

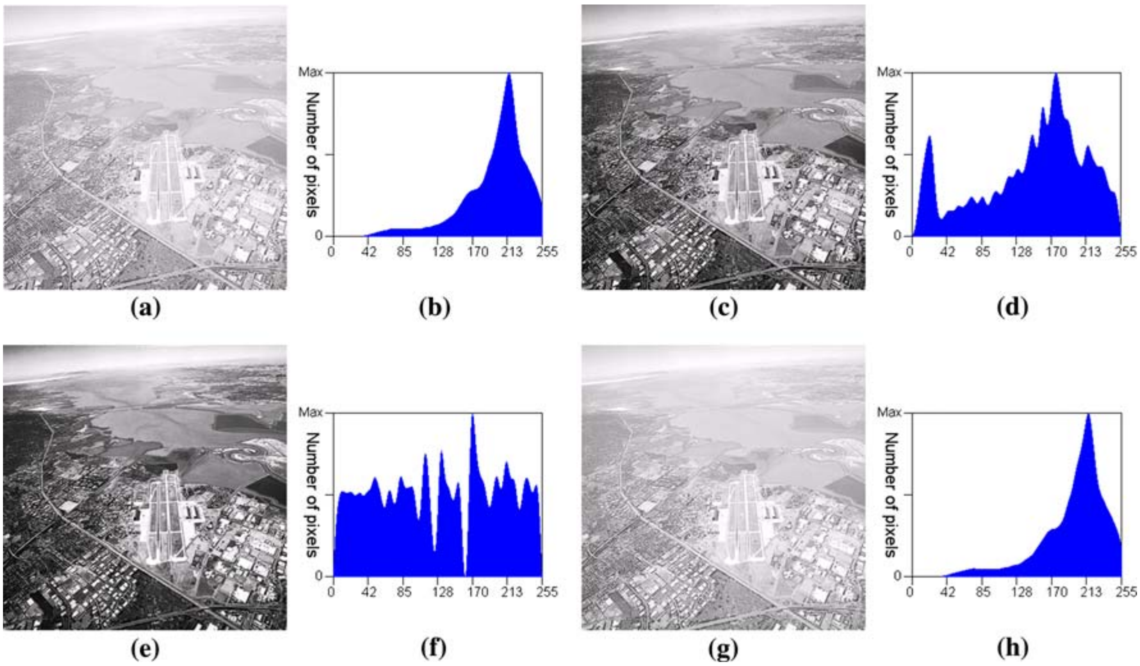

Fig. 17 Enhancement results for Case *F* (mostly bright image). **a** Original image. **b** The histogram of **a**. **c** Enhancement result by our proposal method. **d** The enhancement histogram of **c**. **e** Enhancement result by histogram equalization. **f** The enhancement histogram of **e**. The enhancement result by contrast stretching. **h** The enhancement histogram of **g**

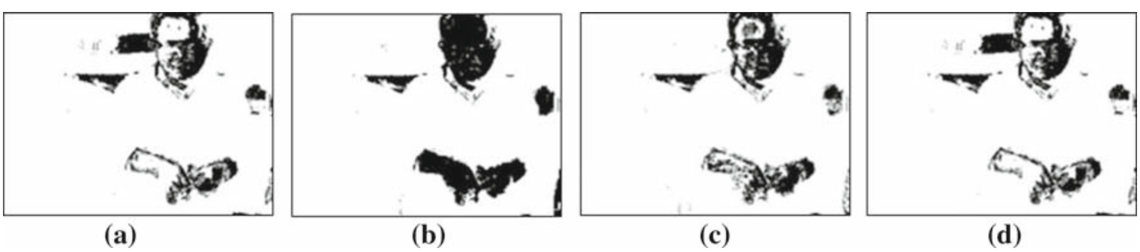

Fig. 18 Skin color detection results for Case *E* (high-contrast image). **a** Original image (Fig. 16a). **b** Enhancement result by our proposal method (Fig. 16c). **c** Enhancement result by histogram equalization (Fig. 16e). **d** Enhancement result by contrast stretching (Fig. 16g)

this figure, we know that the CS cannot enhance the image with mostly bright illumination.

Skin color detections were usually used to be the preprocessing of the face detection. Herein, a skin color detection measurement is proposed to compare with our method, HE, and CS. Wong et al. [21] proposed a skin color detection method which can detect skin color pixels under different illuminations. We modified their skin color detection method to detect the Case *E* images. Figure 18 shows the results by the skin color detection. The skin color pixels are displayed by black and the non-skin color pixels are displayed by white. The skin color of the original (non-enhancement) image (Fig. 16a), our enhanced result (Fig. 16c), HE's result (Fig. 16e), and CS's result (Fig. 16g) performed by the skin color detection are shown in Fig. 18a–d, respectively. The skin color of the forehead, right face, and right hand cannot be detected for the original image and CS. HE's result obtained from the skin color detection can show skin color at forehead, right face, and right hand. However, this result is still not good for face detection. Our enhanced method can detect more skin color pixels than the original image, HE, and CS do. Thus, our proposal enhancement method is proved to be effective by the skin color detection measurement.

In order to prove that our proposal image enhancement is effect, some ground truth color images with high-contrast illumination are used in Case *E*. Adobe Photo CS (Adobe Systems Incorporated [22]) commercial image processing software is used to adjust the illumination value in 100

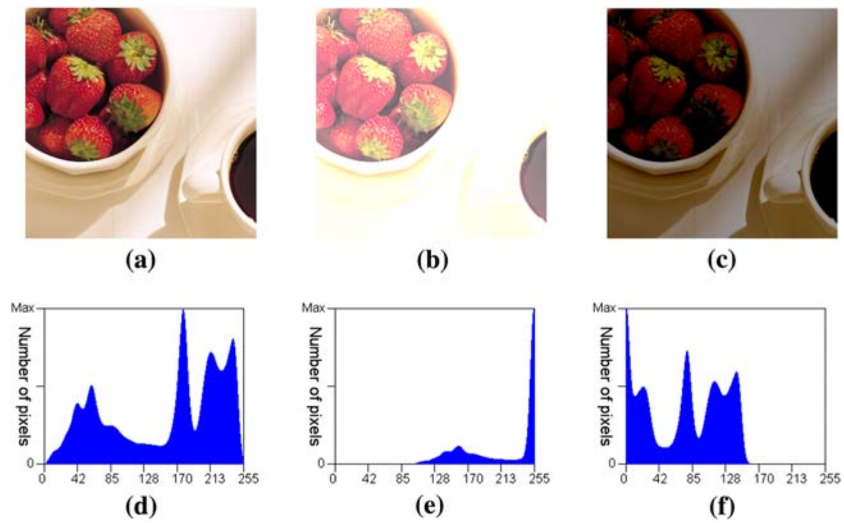

Fig. 19 An example for the ground truth image and artificial image. **a** Ground truth image (Case *E* with high-contrast). **b** The illumination of the ground truth image is increased 100 by Adobe Photoshop software. **c** Illumination decreased 100. **d** Histogram of **a**. **e** Histogram of **b**. **f** Histogram of **c**

increments and in 100 decrements. Further, these adjusted illumination color images are processed by our proposal method, the HE, Adobe Photoshop software, and CS, respectively, and their results are compared to determine which method is better. Here, we propose a measurement method, direct image subtraction method, to be the measurement criterion. The direct image subtraction method is defined as follows

$$DSMQER = \frac{\sum_{y=0}^{\text{Height}-1}\sum_{x=0}^{\text{Width}-1} Sqrt\{(GR_{x,y}-ER_{x,y})^2+(GG_{x,y}-EG_{x,y})^2+(GB_{x,y}-EB_{x,y})^2\}}{\text{Height}\cdot\text{Width}}\% \qquad (7)$$

where $DSMQER$, $GR_{x,y}$, $GG_{x,y}$, $GB_{x,y}$, $ER_{x,y}$, $EG_{x,y}$, and $EB_{x,y}$ are the mean square root error rate of a direct image subtraction, the red component of a ground truth image, the green component of a ground truth image, the blue component of a ground truth image, the red component of a enhancement image, the green component of a enhancement image, and the blue component of a enhancement image, respectively. The value of the *DSMQER* is small if the enhancement image is more equal to a ground truth image.

Herein, we use ten ground truth images, ten artificial images which are processed manually by Adobe Photoshop CS software with illumination value in 100 increments, and ten artificial images with illumination value in 100 decrements by a similar approach. Figure 19 shows an example for a ground truth image and an artificial image with illumination value in 100 increments and 100 decrements, respectively. These artificial images are processed by our proposal method, HE, Adobe Photoshop CS software, and CS, respectively. Further, the direct image subtraction method is used to measure the enhancement performance.

For the images with illumination value in 100 increments are enhanced by our proposed enhancement method, HE, Adobe Photoshop CS, and CS, respectively. The results of the average image subtraction rate obtained from the different methods are shown in Table 3. From this table, our method is better than other methods in image subtraction methods.

Figure 20 shows an example for the enhancement results of the artificial image (Fig. 19b) with illumination value in 100 increments which is enhanced by our enhancement method, HE, Adobe Photoshop CS, and CS, respectively. Making a comparison of Fig. 20b, d, f, h, it shows that Fig. 20b is darker then other methods. That is, our method is better than other methods in brighter image.

For images with illumination value in 100 decrements are enhanced by our enhancement method, HE, Adobe Photoshop CS, and CS, respectively. The average image subtraction rates of the different methods are shown in Table 4. From this table, both our enhancement method and Adobe Photoshop CS software have the similar rates in the image subtraction method.

Table 3 Comparison of the average image subtraction rate for increment illumination images

Methods to enhance increment illumination image	*DSMQER*
Our enhancement method	15.5629
Histogram equalization	30.7219
Adobe Photoshop	35.3669
Contrast stretching	42.6162

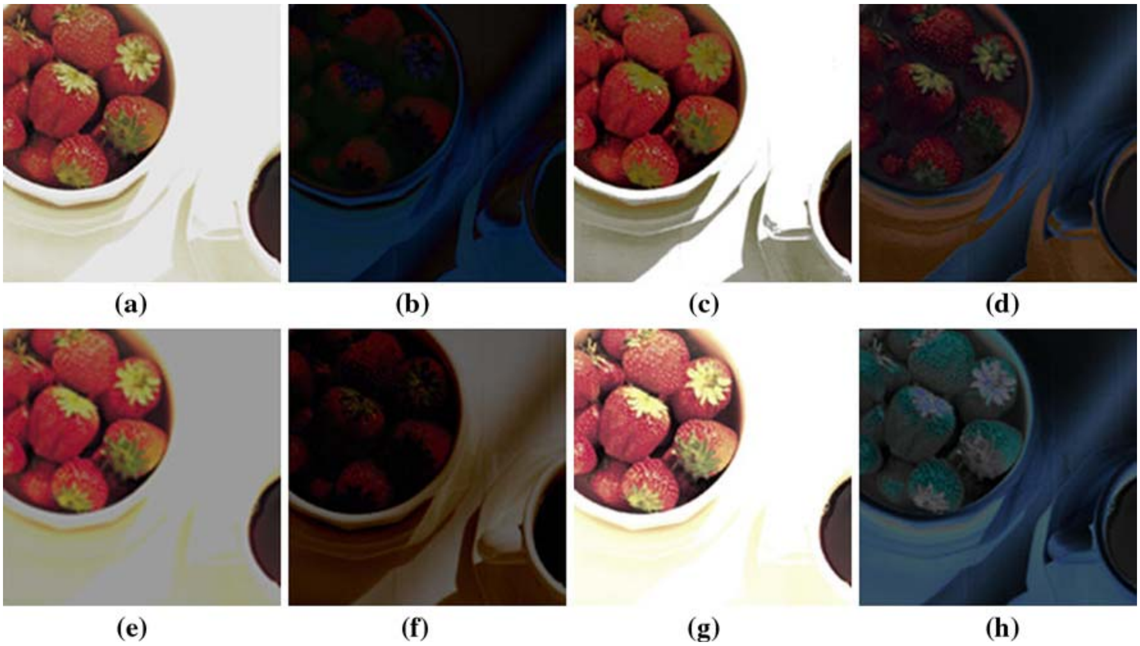

Fig. 20 Enhancement results for artificial image with illumination increased 100. **a** Our result. **b** Color image subtraction result between Figs. 19a and 20a. **c** Histogram equalization result. **d** Color image subtraction result between Figs. 19a and 20c. **e** Adobe Photoshop result. **f** Color image subtraction result between Figs. 19a and 20e. **g** Contrast stretching result. **h** Color image subtraction result between Figs. 19a and 20g

Table 4 Comparison of the average image subtraction rate for decrement illumination images

Methods to enhance decrement illumination image	*DSMQER*
Our enhancement method	17.0076
Histogram equalization	30.8457
Adobe Photoshop	17.0371
Contrast stretching	38.7316

The enhancement results of the artificial image (Fig. 19c) with illumination value in 100 decrements are shown in Fig. 21. Observing these figures, the HE cannot make satisfactory enhancement at brighter illumination. Adobe Photoshop CS software has satisfactory enhancement at brighter illumination but has not satisfactory enhancement at dark illumination. In the Adobe Photoshop CS software's enhanced image, the strawberry's color is brighter, and the coffee's color is brighter too. Generally speaking, the whole image is brighter. The enhancement result of our proposal method is better than those of other methods at bright illumination and dark illumination.

The performance comparison with local enhancement method, such as Meylan's [15] color image enhancement method, is also presented in the experiments. Figure 22a–c depicts the tree image treated with gamma-encoded, Meylan's method, and our method, respectively. From these images, we can find that our results are better than Meylan's result at the shadow. Figure 22d–f depicts the auto image treated with gamma-encoded, Meylan's method, and our method, respectively. From these images, we can find that our results are clearer than Meylan's result at the shadow, the door, and bikes. Furthermore, our global enhancement method is more efficient than Meylan's surround-based Retinex method.

Figure 23 presents several fail enhancement results of face images. The face images are obtained from Yale Face Database B. Figure 23a depicts the "yaleB08_P00A-110E+65.jpg" image. This image has eyes with too dark illumination. After applied our image enhancement, the result is shown in Fig. 23b. Our proposal method cannot make the eyes clearly. Another face image "yaleB02_P00A+095E+00.jpg" (Fig. 23c) contain the facial features which their illumination is too dark. This image is enhanced by our method, and the result is shown in Fig. 23d. Thus, this kind of images needs more effective enhancement technique to improve.

6 Conclusions and future works

This study has presented a decision tree-based, automatic, and parameter-free contrast enhancement method for various color images. The content of the input image was analyzed first. And the statistical features are extracted to be

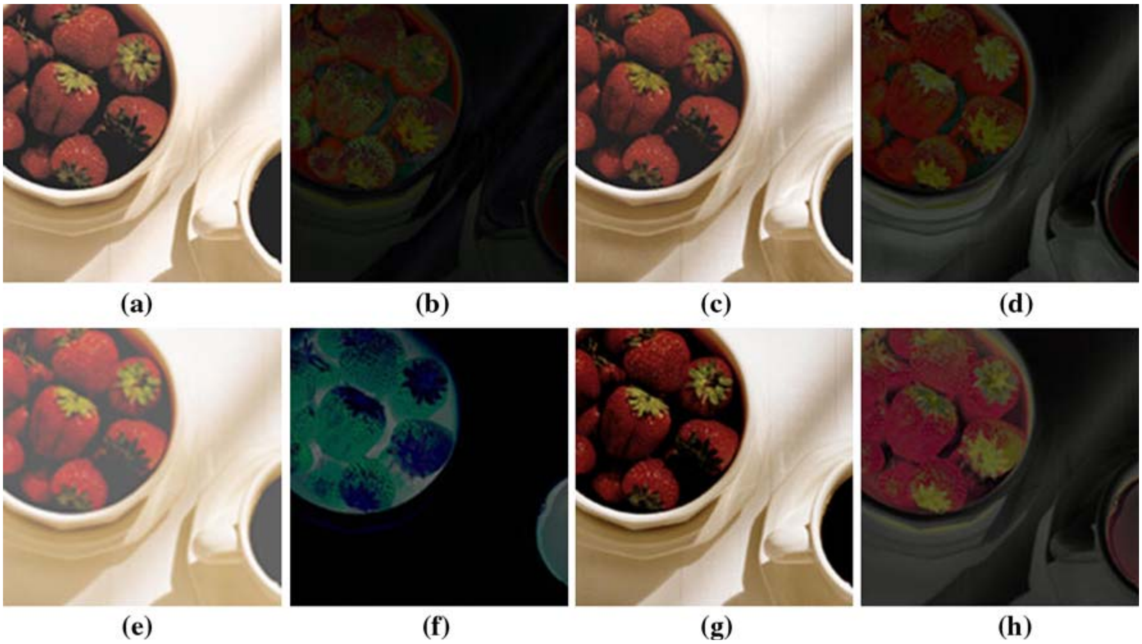

Fig. 21 Enhancement results for artificial image with illumination decreased 100. **a** Our result. **b** Color image subtraction result between Figs. 19a and 21a. **c** Histogram equalization result. **d** Color image subtraction result between Figs. 19a and 21c. **e** Adobe Photoshop result. **f** Color image subtraction result between Figs. 19a and 21e. **g** Contrast stretching result. **h** Color image subtraction result between Figs. 19a and 21g

Fig. 22 Results of comparison with local enhancement method. **a** Tree gamma-encoded image. **b** Treated with Meylan's method. **c** Treated with our method. **d** Auto gamma-encoded image. **e** Treated with Meylan's method. **f** Treated with our method

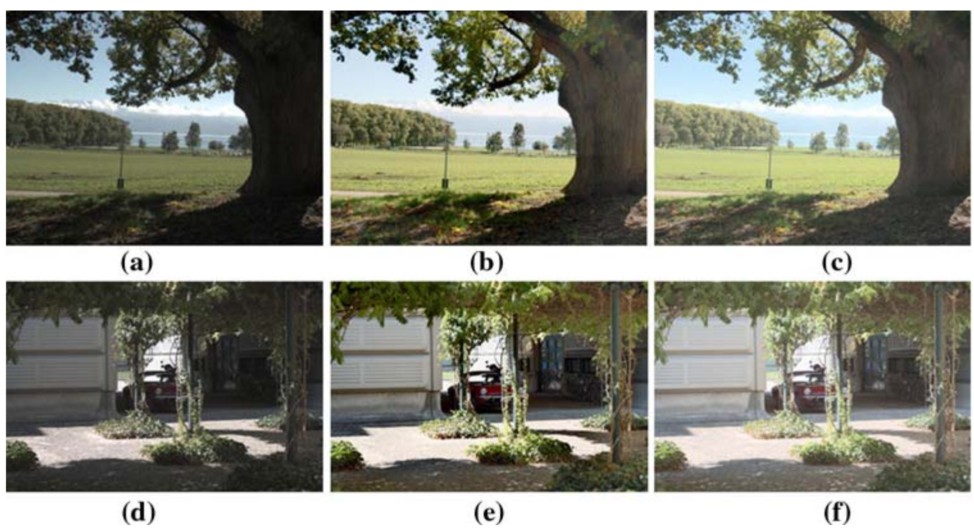

used to classify the testing image into one of dark, low-contrast, bright, mostly dark, high-contrast, and mostly bright class. Then, a decision tree was employed to decide the input images which class it belongs to. For each image class, the image content distribution (each luminance distribution is represented by one peak and two valleys) is obtained by analyzing the luminance histogram. The parameters of the PLT are specified by the image content distribution (peaks and valleys). The proposed method is tested on various kinds (face image, license plate, bio-image, aerial image, optical image, scenery…, etc.) of color images and gray level images. The performance analysis (by skin detection, visual, and image subtraction) indicated that our method is very efficient and effective by comparing with HE, Adobe Photoshop CS software, and CS.

To obtain satisfactory enhancement results and processing speed, future works should focus on the following: (1) Optimize our program; (2) Apply our proposal method to particular applications; (3) Propose more objective and effective enhancement measurement; (4) Process the image which

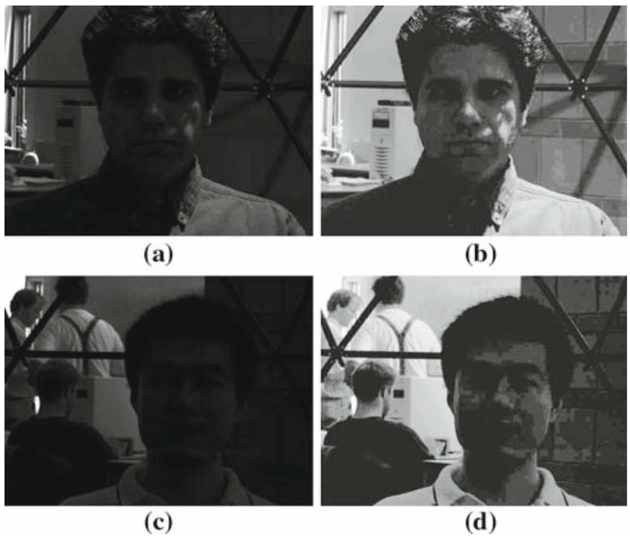

Fig. 23 Three examples, which are unsolvable by ours as well as other comparison methods. **a** Face image one, "yaleB08_P00A-110E+65.jpg", with the dark illumination of the eyes. **b** Our result is not clear in eyes for **a**. **c** Face image two, "yaleB02_P00A+095E+00.jpg", with the dark illumination of the facial features. **d** The facial features of our result are obvious for **c**

has foreground objects with darker illumination and low illumination.

Acknowledgments This work was supported by the Ministry of Economic, R.O.C., under Grants MOEA-96-EC-17-A-02-S1-032 and National Science Council, R.O.C., under Grants NSC 96-2221-E-133-001-.

References

1. Gonzalez, R.C., Woods, R.E.: Digital Image Processing, 2nd edn. Prentice-Hall, Englewood Cliffs (2002). http://www.imageprocessingplace.com
2. Gonzalez, R.C., Woods, R.E., Eddins, S.L.: Digital Image Processing Using MATLAB. Prentice-Hall, Englewood Cliffs (2004). http://www.imageprocessingplace.com
3. Naik, S.K., Murthy, C.A.: Hue-preserving color image enhancement without gamut problem. IEEE Trans. Image Process. **12**(12), 1591–1598 (2003)
4. Strickland, R.N., Kim, C.S., Mcdonnell, W.F.: Digital color image enhancement based on the saturation component. Opt. Eng. **26**(7), 609–616 (1987)
5. Thomas, B.A., Strickland, R.N., Rodriguez, J.J.: Color image enhancement using spatially adaptive saturation feedback. In: Proceedings of the International Conference on Image Processing, vol. 3, pp. 30–33 (1997)
6. Yang, C.C., Rodriguez, J.J.: Efficient luminance and saturation processing techniques for color images. J. Vis. Commun. Image Represent. **3**(3), 263–277 (1997)
7. Yang, C.C., Kwork, S.H.: Efficient gamut clipping for color image processing using LHS and YIQ. Opt. Eng. **42**(3), 701–711 (2003)
8. Pei, S.C., Zeng, Y.C., Chang, C.H.: Virtual restoration of ancient Chinese paintings using color contrast enhancement and Lacuna texture synthesis. IEEE Trans. Image Process. **13**(3), 416–429 (2004)
9. Tan, K.K., Oakley, J.P.: Physics-based approach to color image enhancement in poor visibility conditions. J. Opt. Soc. Am. A **18**(10), 2460–2467 (2001)
10. Hanmandlu, M., Jha, D., Sharma, R.: Color image enhancement by fuzzy intensification. In: Proceedings of the 15th International Conference on Pattern Recognition, vol. 3, pp. 310–313 (2000)
11. Mlsna, P.A., Rodriguez, J.J.: A multivariate contrast enhancement technique for multispectral images. IEEE Trans. Geosci. Remote Sens. **33**(1), 212–216 (1995)
12. Duan, J., Qiu, G.: Novel histogram processing for colour image enhancement. In: Proceedings of the Third International Conference on Image and Graphics, pp. 55–58 (2004)
13. Sun, C.C., Ruan, S.J., Shie, M.C., Pai, T.W.: Dynamic contrast enhancement based on histogram specification. IEEE Trans. Consumer Electron. **51**(4), 1300–1305 (2005)
14. Chatterji, B.N., Murthy, N.R.: Adaptive contrast enhancement for color images. In: Proceedings of 1997 International Conference on Information, Communications and Signal Processing, vol. 3, pp. 1537–1541 (1997)
15. Meylan, L., Süsstrunk, S.: Color image enhancement using a retinex-based adaptive filter. In: Proceedings of the IS&T Second European Conference on Color in Graphics, Image, and Vision (CGIV 2004), vol. 2, pp. 359–363 (2004)
16. Munteanu, C., Rosa, A.: Color image enhancement using evolutionary principles and the retinex theory of color constancy. In: Neural Networks for Signal Processing XI, 2001. Proceedings of the 2001 IEEE Signal Processing Society Workshop, pp. 393–402 (2001)
17. Tsai, C.M., Lee, H.J.: Binarization of color document images via luminance and saturation color features. IEEE Trans. Image Process. **11**(4), 434–451 (2002)
18. Tsai, D.M.: A fast thresholding selection procedure for multimode and unimodel histograms. Pattern Recognit. Lett. **16**, 653–666 (1995)
19. Asayama, Y., Miyamoto, S., Oi, K., Ikebe, Y.: Least square method for enhancement of laser radar images based on piecewise linear transformations of gray scales, Acoustics, Speech, and Signal Processing. IEEE Int. Conf. ICASSP '86 **11**, 1513–1516 (1986)
20. Georghiades, A.S., Belhumeur, P.N., Kriegman, D.J.: From few to many: illumination cone models for face recognition under variable lighting and pose. IEEE Trans. Pattern Anal. Mach. Intell. **23**(6), 643–660 (2001). http://cvc.yale.edu/projects/yalefacesB/yalefacesB.html
21. Wong, K.W., Lam, K.M., Siu, W.C.: A robust scheme for live detection of human faces in color images. Signal Process. Image Commun. **18**(2), 103–114 (2003)
22. Adobe Systems Incorporated, Adobe Photoshop CS. http://www.adobe.com/products/photoshop/main.html?c=us

Author biographies

Chun-Ming Tsai was born in Taipei, Taiwan, in 1963. He received the B.S. degree in Industrial Education with major in electrical engineering from National Taiwan Normal University, Taipei, Taiwan, in 1988. He received the M.S. and the Ph.D. degree in Computer Science and Information Engineering from National Chiao Tung University, Hsinchu, Taiwan, in 1996 and 2002, respectively. He was a visiting scholar in Department of Computer Science, University of California Santa Barbara, California, USA, August 2005–July 2006. Dr. Tsai joined the faculty of National Tam-Shui Vocational High School, Taipei, Taiwan in August 1987. August 2003, Dr. Tsai joined the faculty of Taipei Municipal Teacher College (TMTC), Taipei, Taiwan. He was an assistant professor in the Department of Mathematics and Computer Science Education, Taipei Municipal University of Education (TMUE) from August 2006 to July 2007. He was an assistant professor in the Department of Computer Science, Taipei Municipal University of Education (TMUE) from August 2007 to July 2008. He is currently an associate professor in the Department of Computer Science, Taipei Municipal University of Education (TMUE). His research interests include Video and Image Processing (VIP), Machine Learning (ML), Medical Image Processing (MIP), Document Image Analysis (DIA), and Brain Computer Interface (BCI).

Zong-Mu Yeh received the M.S. degree in electronics engineering from the National Taiwan University of Science and Technology, Taipei, Taiwan in 1982 and Ph.D. degree in industrial technology from Iowa State University, Iowa, in 1992. He is currently a professor in the department of mechatronic technology of National Taiwan Normal University (NTNU). His research interests include brain computer interface, fuzzy logic, digital signal processing and E-learning.

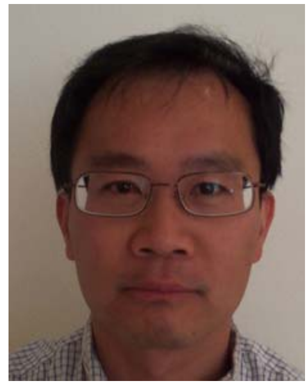

Yuan-Fang Wang received his Ph.D. degrees in electrical and computer engineering from the University of Texas at Austin. He is a Professor with the Department of Computer Science at the University of California at Santa Barbara. His research activities center around computer vision, computer graphics, and pattern recognition. Dr. Wang served on many program committees and chaired numerous technical sessions at professional meetings. He was a Program Chair of the IEEE CVPR conference in 1998 and an Associate Editor of IEEE PAMI from 1998 to 2002. He co-founded the first ACM Workshop on Video Surveillance in 2003, co-chaired the second and the third ACM Workshop on Video Surveillance and Sensor Networks in 2004 and 2005. Dr. Wang was a guest editor of a special issue on video surveillance in the ACM Multimedia Systems Journal in 2004. Dr. Wang has received funding support from many federal agencies including NSF, NASA, DARPA, Army, and Navy, and also from private industries. He has published over 100 refereed journal and conference papers in computer vision, computer graphics, pattern recognition, and robotics.